High-spin Structure Studies in 62Zn

Gellanki, Jnaneswari; Rudolph, Dirk; Ragnarsson, Ingemar; Andersson, Lise-Lotte; Andreoiu, Corina; Carpenter, M. P.; Ekman, Jörgen; Fahlander, Claes; Johansson, Emma; Reviol, W.; Sarantites, D. G.; Seweryniak, D.; Svensson, C. E.

Published in:
Physica Scripta

DOI:
10.1088/0031-8949/2012/T150/014013

2012

LUND UNIVERSITY

PO Box 117
221 00 Lund
+46 46-222 00 00

High spin structure studies in ^{62}Zn

J. Gellanki,[1] D. Rudolph,[1] I. Ragnarsson,[2]
L.-L. Andersson,[1,‡] C. Andreoiu,[1,3,§] M. P. Carpenter,[4]
J. Ekman,[1,‖] C. Fahlander,[1] E. K. Johansson,[1] W. Reviol,[5]
D. G. Sarantites,[5] D. Seweryniak,[4] C. E. Svensson,[3]

[1] Department of Physics, Lund University, Lund, Sweden
[2] Division of Mathematical Physics, LTH, Lund University, Lund, Sweden
[3] Department of Physics, University of Guelph, Canada
[4] Physics Division, Argonne National Laboratory, U.S.A.
[5] Chemistry Department, Washington University, St. Louis, U.S.A.

E-mail: `gellanki.jnaneswari@nuclear.lu.se`

Abstract. A detailed experimental study of the ^{62}Zn nucleus has been performed by combining the data sets from four fusion-evaporation reaction experiments. Apart from the previously published data, the present results include some ten new rotational band structures and one new superdeformed band. The GAMMASPHERE Ge-detector array in conjunction with the 4π charged-particle detector array Microball allowed for the detection of γ-rays in coincidence with evaporated light particles. The deduced level scheme includes some 250 excited states, which are connected with 430 γ-ray transitions. The multipolarities have been assigned via directional correlations of γ-rays emitted from oriented states. The experimental characteristics of the rotational bands are analyzed and compared with results from Cranked Nilsson-Strutinsky calculations.

PACS numbers: 21.60.Cs, 23.20.En, 23.20.Lv, 27.50.+e

Submitted to: *Phys. Scr.*

1. Introduction

In recent years, modern germanium detector arrays like GAMMASPHERE [1] in conjunction with the charged particle arrays such as Microball [2] have been used to identify nuclear structure properties at high spin in the $A \sim 60$ mass region, like band termination, highly deformed bands, superdeformed bands, prompt proton decays and shape changes [3, 4, 5, 6, 7, 8, 9, 10, 11, 12, 13, 14, 15, 16, 17, 18, 19]. An interesting feature in this mass region is that the same nuclei can exhibit various kinds of the above mentioned nuclear phenomena [6, 10, 13, 18, 20]. To generate the high-spin states required for the observation of most of the collective phenomena, it is necessary to break the $Z = N = 28$ core and to excite nucleons into the intruder $1g_{9/2}$ subshell.

‡ Present address: Helmholtz-Institut Mainz, D-55099 Mainz, Germany.
§ Present address: Chemistry Department, Simon Fraser University, Burnaby, BC, V5a 1S6, Canada.
‖ Present address: Malmö högskola, S-20506 Malmö, Sweden.

2. Experimental Details

The low-lying states in ^{62}Zn including two terminating bands and one unlinked superdeformed band were established in previous studies [16, 17]. Three superdeformed bands were resolved in our recent study [21]. The combined statistics of four different experiments performed at Argonne and Lawrence Berkeley National Laboratories were used to identify the excited states of ^{62}Zn. Detailed description of these experiments are given in [6, 8, 10, 13, 14]. The first experiment which has high counting statistics used the fusion-evaporation reaction ^{40}Ca(^{28}Si,1α2p)^{62}Zn at a beam energy of 122 MeV. The target had a thickness of 0.5 mg/cm^2 and an isotopic enrichment of 99.975%. The relative population cross section for ^{62}Zn was $\sim$ 30%. The other three experiments utilized the fusion-evaporation reaction ^{28}Si(^{36}Ar,2p)^{62}Zn at similar beam energies, $\sim$ 140 MeV, leading to a small population cross section for ^{62}Zn. All four experiments used the 4π Ge-detector array GAMMASPHERE [1] combined with the particle detector Microball [2]. The statistics from the first experiment was used to identify the normally deformed, well deformed, and superdeformed band structures including their decay-out transitions. The combined statistics of the remaining three experiments was used to add the highest-spin states on top of the superdeformed bands. In all experiments the heavimet collimators in front of the Ge detectors were removed to provide γ-ray multiplicity and sum-energy measurements [22] and additional channel selectivity by total energy conservation requirements [23].

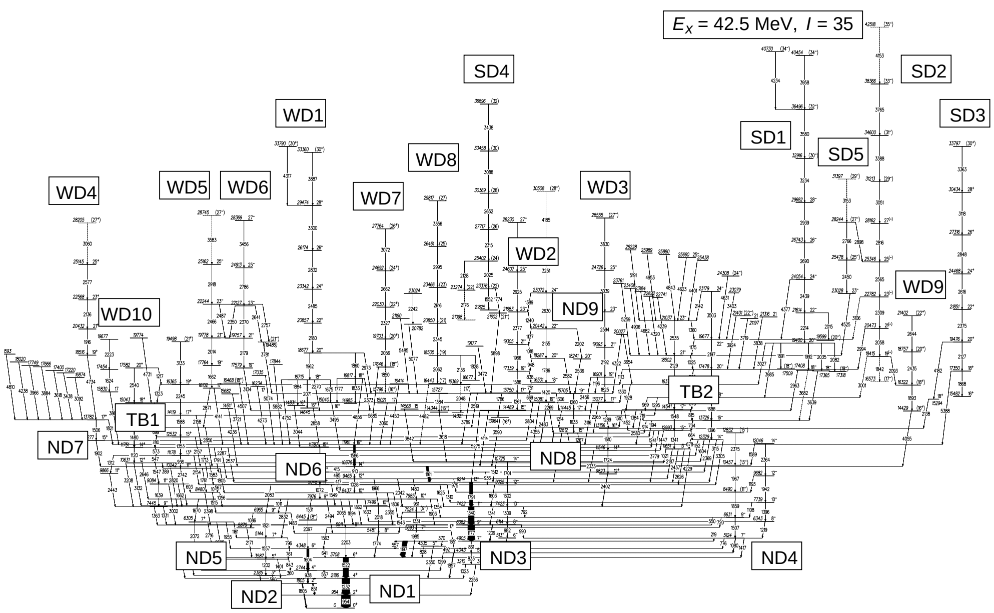

Figure 1. Overview of the complex level scheme of ^{62}Zn as obtained in the present study. The various normal deformed (ND), terminating (TB), well-deformed (WD), and superdeformed (SD) bands are labeled.

3. Analysis and Results

The γ-ray events were sorted offline into various γ-ray energy projections, $E_\gamma - E_\gamma$ matrices, and $E_\gamma - E_\gamma - E_\gamma$ cubes subject to appropriate evaporated particle conditions. Analysis of the cube and the matrices was carried out using the RADWARE software package [24] and the spectrum-analysis code Tv [25]. A kinematic correction [26, 27] was used to aid in the Doppler correction. The assignment of multipolarities to the γ-rays was done by using directional correlations from the oriented states (DCO ratios).

The current results confirm the previous results for the lower-spin states and reveal much more information at high spin. The complete level scheme deduced for ^{62}Zn is indicated in Fig. 1. Since it comprises about 430 γ-ray transitions and 250 excited states, its detailed presentation is subject to an extensive study in a forthcoming publication [20]. To ease the discussion, the level scheme is classified into normal deformed structures (ND1-ND9), the known terminating bands (TB1,TB2) [17], as well as a number of well-deformed (WD1-WD10) and superdeformed (SD1-SD5) bands in Fig. 1. The level energies, the corresponding depopulating γ-rays, their relative intensities, angular-correlation ratios, and resulting spin-parity assignments are summarized in Ref. [20].

The highest spin deduced from a connected band in the previous study is 24^- at 23214 keV [17]. Our recent publication [21] focused on three superdeformed bands and one well deformed band, where the observed maximum spin is (35^-) at 42.5 MeV excitation energy. The present level scheme in Fig. 1 adds a few new low-spin normal deformed structures, nine well-deformed bands (WD2-WD10), and two superdeformed bands (SD4,SD5). Some structures (e.g. WD2) consist of two signature partner bands, which will be denoted with (a) and (b) in addition to the band label.

All highly deformed rotational structures were identified up to $I \sim$ 25-28 $\hbar$ whereas the superdeformed bands were observed up to $I \sim$ 30-35 $\hbar$. Most of the excited rotational bands were connected to the low-spin normal deformed states by a number of linking transitions. In most cases, this allowed for firm, but sometimes only tentative spin and parity assignments to the lowest states in the bands. For example, the lowest state at 16102 keV of WD5 decays into the normal deformed 16^+ state at 11961 keV via a 4141-keV decay-out transition. The $R_{DCO}(4141) = 0.51(10)$ is consistent with $\Delta I = 1$ character, suggesting $I = 17$ to the 16102-keV state. The tentative spin and parity assignments to the states near the top of the bands are based on their regular rotational behaviour.

A spectrum in coincidence with the 4355 keV decay-out transition of WD2b and any one of the band members of WD2b (1420, 1786, 2155 and 2630 keV) is shown in Fig. 2. It illustrates the high sensitivity of the first experiment, with small relative yields such as 0.04% for the gating 4355 keV transition and about 2% for the band members. The triple coincidences both with band members of WD2b (1420, 1786, 2155, 2630, and 3251 keV) and with the relevant transitions in the normal deformed region (954, 1177, 1197, 1232, 1309, 1340, 1341, 1512, 1522, 1602-1604, and 1701 keV) are clearly visible. The weak connecting transitions 838 and 1018 keV between signature partner bands WD2a and WD2b are also marked. The peak at 2925 keV belongs to WD2a. The presence of a 2355-keV peak marked in red is related to contamination arising from the intense, yrast $13^- \rightarrow 11^-$ 1791-keV γ-ray transition, which has nearly the same energy as the band member at 1786 keV.

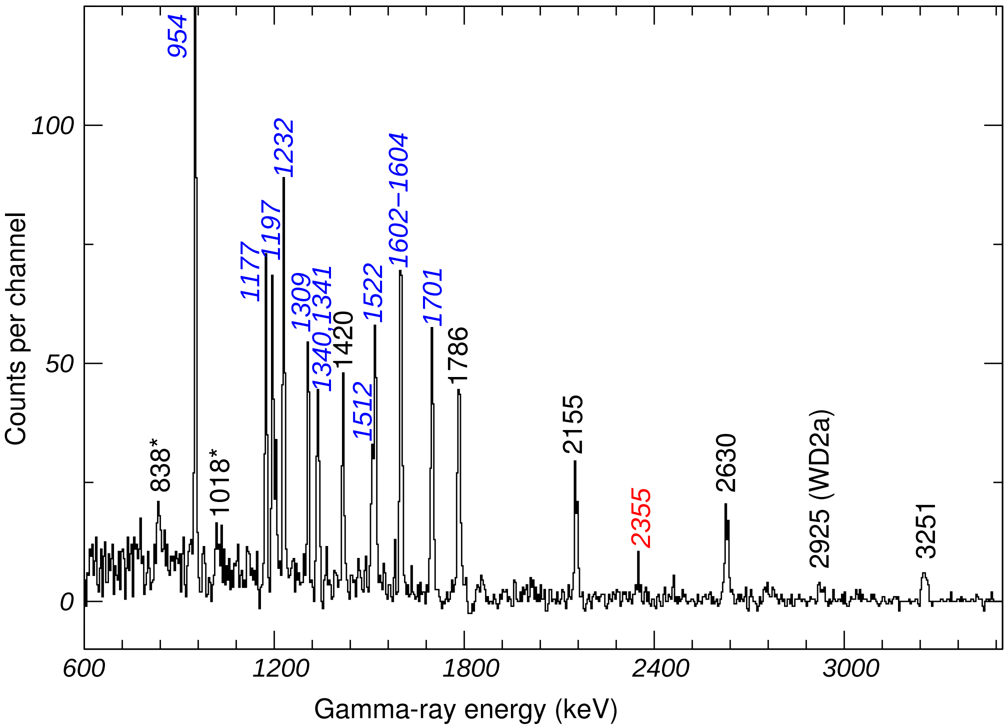

Figure 2. Coincidences with the 4355-keV decay-out transition of WD2b and any one of the band members of WD2b at 1420, 1786, 2155, and 2630 keV. Transitions from the normal deformed part of the level scheme are marked in blue and italic style, while the band members including the 2925 keV transition of WD2a are marked in black. The transitions at 838 and 1018 keV connecting WD2a and WD2b are marked with a star (*). The peak at 2355 keV is a contaminant.

4. Theoretical Interpretations

The experimental bands were analyzed using the configuration-dependent cranked Nilsson-Strutinsky (CNS) model [28, 29, 30]. These calculations are based on the cranking model [31, 32], with the single-particle eigenvalues calculated from the Nilsson Hamiltonian [28]. The total energy of fixed configurations is minimized in the deformation parameters ϵ_2, γ and ϵ_4 at each spin. Pairing effects are neglected since the formalism has been developed to describe the high-spin structures.

The orbitals involved for a description of ^{62}Zn include those of the $\mathcal{N} = 3$ high-j $1f_{7/2}$ shell, the upper fp shell comprising $1f_{5/2}$, $2p_{3/2}$ and $2p_{1/2}$, and finally the $\mathcal{N} = 4$ $1g_{9/2}$ shell. The configurations are labeled $[p_1p_2,n_1n_2]$, where p_1 (n_1) is the number of proton (neutron) holes in the $1f_{7/2}$ subshell and p_2 (n_2) is the number of proton (neutron) particles in the $1g_{9/2}$ shell. For example, the ground-state band configuration $\pi(2p_{3/2}1f_{5/2})^2\nu(2p_{3/2}1f_{5/2})^4$ of ^{62}Zn is labeled as [00,00]. In order to form regular rotational bands, it is necessary to lift protons or neutrons across the $Z = N = 28$ spherical shell gaps from the $1f_{7/2}$ shell, while the excitation of particles to the $1g_{9/2}$ shell is important to increase the deformation and to generate angular momentum [10].

In Fig. 3, some of the bands are compared with the CNS predictions. The upper

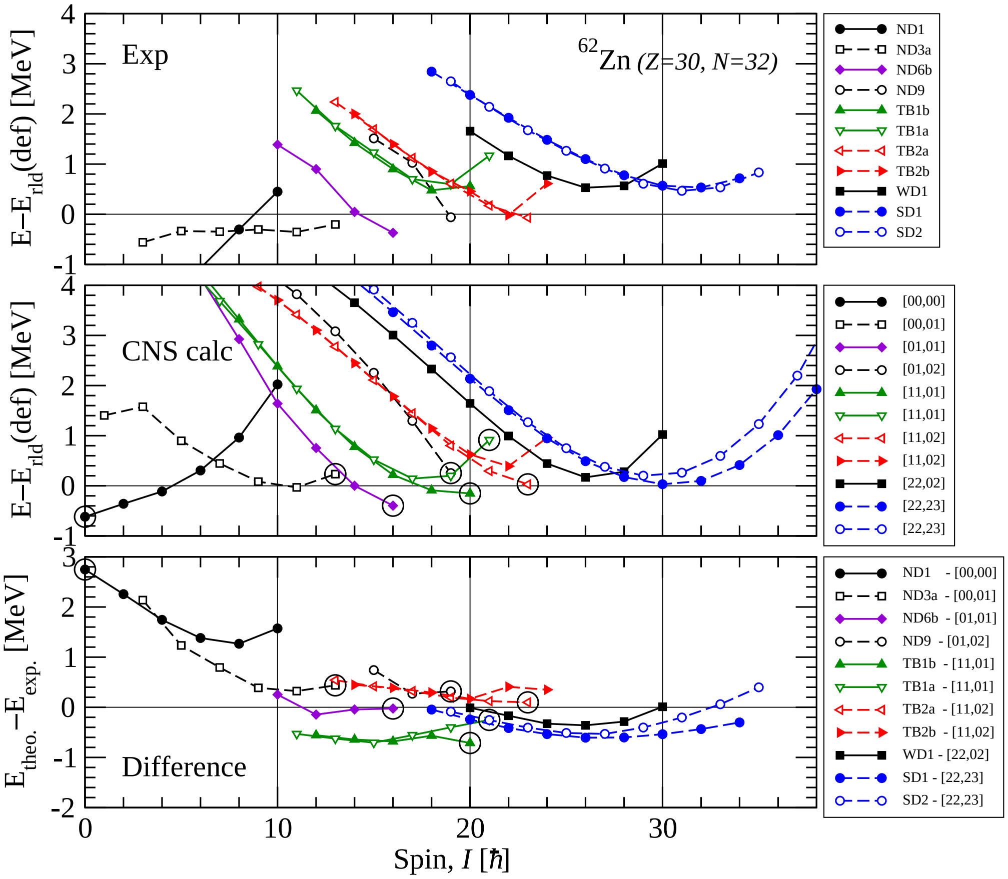

Figure 3. Comparison between some of the observed structures (cf. Fig. 1) and CNS predictions for ^{62}Zn. The top panel illustrates the experimental results where the bands are labeled according to Fig. 1. The middle panel shows the chosen predicted bands. The bottom panel plots the energy difference between the prediction and observation.

panel shows the experimental energies relative to the rotating liquid drop energy. The middle panel shows selected calculated bands, and the lower panel indicates the difference between the experimental and calculated bands. If perfect agreement between the theoretical and experimental bands existed, the values in the lower panel would be equal to zero. One can note that a constant energy difference in the lower panel implies that the experimental transition energies are reproduced by the calculated band. The previously known terminating bands TB1 and TB2 are in agreement with the [11,01] and [11,02] configurations. The well-deformed band WD1 is assigned to the [22,02] configuration, whereas the two superdeformed bands SD1 and SD2 are assigned as signature partners of the [22,23] configuration. The other well-deformed bands (WD2-WD10) are typically formed with three particles in the $1g_{9/2}$ shell and two $1f_{7/2}$ holes, while the superdeformed bands have three to four $1f_{7/2}$ holes and four to six $1g_{9/2}$ particles. More details about the band configurations are discussed in Ref. [20].

References

[1] I.-Y. Lee, Nucl. Phys. **A520**, 641c (1990).
[2] D.G. Sarantites *et al.*, Nucl. Instr. Meth. **A381**, 418 (1996).
[3] W. Reviol *et al.*, Phys. Rev. C **65**, 034309 (2002).
[4] D. Rudolph *et al.*, Phys. Rev. Lett. **96**, 092501 (2006).
[5] E.K. Johansson *et al.*, Phys. Rev. C **77**,064316 (2008).
[6] E.K. Johansson *et al.*, Phys. Rev. C **80**, 014321 (2009).
[7] C.-H. Yu *et al.*, Phys. Rev. C **65**, 061302(R) (2002).
[8] D.A. Torres *et al.*, Phys. Rev. C **78**, 054318 (2008).
[9] D. Rudolph *et al.*, Phys. Rev. Lett. **80**, 3018 (1998).
[10] C. Andreoiu *et al.*, Eur.Phys. J. A**14**, 317 (2002).
[11] C. Andreoiu *et al.*, Phys. Rev. Lett. **91**, 232502 (2003).
[12] C. Andreoiu *et al.*, Phys. Rev. C **62**, 051301(R) (2000).
[13] L.-L. Andersson *et al.*, Eur. Phys. J. A**36**, 251 (2008).
[14] C.E. Svensson *et al.*, Phys. Rev. Lett. **82**, 3400 (1999).
[15] C.-H. Yu *et al.*, Phys. Rev. C **60**, 031305(R) (1999).
[16] C.E. Svensson *et al.*, Phys. Rev. Lett. **79**, 1233 (1997).
[17] C.E. Svensson *et al.*, Phys. Rev. Lett. **80**, 2558(1998).
[18] L.-L. Andersson *et al.*, Phys. Rev. C **79**, 024312 (2009).
[19] D. Karlgren *et al.*, Phys. Rev. C **69**, 034330 (2004).
[20] J. Gellanki *et al.*, submitted to Phys. Rev. C.
[21] J. Gellanki *et al.*, Phys. Rev. C **80**, 051304(R) (2009).
[22] M. Devlin *et al.*, Nucl. Instr. Meth. **A383**, 506 (1996).
[23] C.E. Svensson *et al.*, Nucl. Instr. Meth. **A396**, 288 (1997).
[24] D. C. Radford, Nucl. Instr. Meth. **A361**, 297 (1995).
[25] J. Theuerkauf, S. Esser, S. Krink, M. Luig, N. Nicolay, O. Stuch, H. Wolters, Program Tv, University of Cologne, unpublished.
[26] C.J. Chiara *et al.*, Nucl. Instr. Meth. **A523**, 374 (2004).
[27] D. Seweryniak *et al.*, Nucl. Instr. Meth. **A340**, 353 (1994).
[28] T. Bengtsson and I. Ragnarsson, Nucl. Phys. **A436**, 14 (1985).
[29] A. V. Afanasjev, D. B. Fossan, G. J. Lane, and I. Ragnarsson, Phys. Rep. **322**, 1 (1999).
[30] B. G. Carlsson and I. Ragnarsson, Phys. Rev. C **74**, 011302(R) (2006).
[31] D.R. Inglis, Phys. Rev. **96**, 1059 (1954).
[32] D.R. Inglis, Phys. Rev. **103**, 1786 (1956).